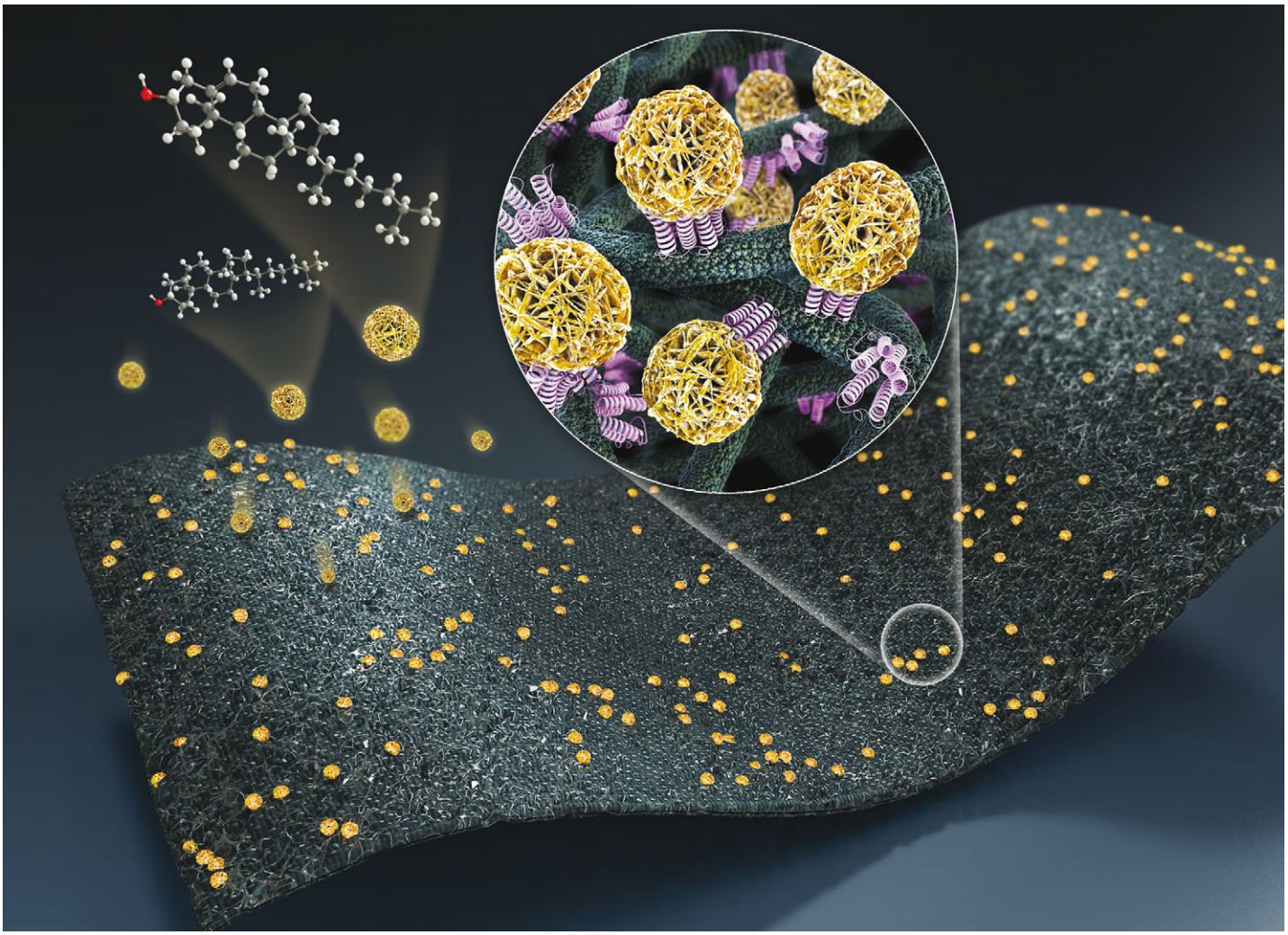

Showcasing research conducted in Dr S. Lee's laboratory at Korea Institute of Science and Technology, Jeonbuk, Republic of Korea, and Prof. V. Gupta's laboratory at University of Delhi, New Delhi, India.

Controllable one step copper coating on carbon nanofibers for flexible cholesterol biosensor substrates

One step coating of CuO nanoparticles on carbon nanofibers has been achieved by a modified hydroxyl ion assisted reduction method. This CuO-coated carbon nanofiber-based flexible platform with physically adsorbed cholesterol oxidase enzyme has further been used for the efficient detection of cholesterol.

As featured in:

See Vinay Gupta, Sungho Lee *et al.*, *J. Mater. Chem. B*, 2016, **4**, 229.

ROYAL SOCIETY OF CHEMISTRY

www.rsc.org/MaterialsB

Registered charity number: 207890

Journal of
Materials Chemistry B

PAPER

View Article Online
View Journal | View Issue

Cite this: J. Mater. Chem. B, 2016, 4, 229

Controllable one step copper coating on carbon nanofibers for flexible cholesterol biosensor substrates†

Bharat Bajaj,[ab] Han I. Joh,[a] Seong M. Jo,[ac] Gurpreet Kaur,[d] Anjali Sharma,[d] Monika Tomar,[e] Vinay Gupta*[d] and Sungho Lee*[ac]

Received 28th August 2015,
Accepted 22nd November 2015

DOI: 10.1039/c5tb01781e

www.rsc.org/MaterialsB

Electrospun carbon nanofibers (CNFs) decorated with copper oxide nanoparticles were successfully synthesized using a one step and modified hydroxyl ion assisted alcohol reduction method. The X-ray diffraction pattern reveals the presence of (−111), (111) and (−202) crystal planes of monoclinic copper oxide (CuO). The CuO coated CNF air annealed at 250 °C exhibited an electrical conductivity of 251 S m^{-1}. The CuO coated CNFs were employed as a novel flexible matrix for a cholesterol biosensor. The biosensor exhibited a high sensitivity of 75 μA mM^{-1} cm^{-2} over the linear range (0.12 mM to 12.93 mM) of cholesterol. This coating method offers easy and inexpensive processing with a flexible and robust supporting structure for biosensing applications.

Introduction

Currently, nanostructured materials have attracted considerable attention because of their excellent efficiency for various technological applications in comparison with the bulk or micro-sized counterparts.[1,2] In particular one dimensional carbon nanostructures such as nanowires, nanofibers, nanotubes, *etc.*, possess superior chemical, electrical, and mechanical properties, which in combination with their high surface-to-volume ratios facilitate the development of various hybrid devices.[2–4] Among these carbon nanostructures, carbon nanofibers (CNFs) are very promising materials[5] for their potential applications in hydrogen energy storage,[6] lithium-ion rechargeable batteries (LIBs),[7] fuel cells,[8] and electrochemical double-layer capacitors (EDLCs)[9] and can also serve as an excellent matrix for biosensing applications.[10] Furthermore, metallization and functionalization using CNFs are effective gateways for improving the performance of biosensors. CNFs can serve as an excellent immobilization matrix for the attachment of a desired biomolecule to their surface owing to their biocompatibility as well as flexibility.[11]

Flexible substrates are light weight, robust, capable of being folded for storage, can attach to uneven surfaces and are promising for the development of implantable biosensors.[12] Carbon based materials[13] such as CNFs can be used as flexible supports for the deposition of metal oxide nanoparticles and provide an added advantage for biosensing applications. Metallic coatings on the surface of carbon based materials were obtained using chemical vapor deposition (CVD) and a wet chemical process.[3,14,15] However, coating of homogeneous and facile metals and their oxide nanoparticles directly on the surface of CNFs is very challenging.[16] Therefore, many studies have been conducted on the coating of metal or metal oxides on the CNF surface by functionalization and other techniques.[17–19] Oxidative acid treatment is one of the approaches for the generation of functional groups on the CNF surface. In the coating, the density of surface functional groups required for uniform metal deposition and interaction is severely affected using the above technique.[20–25] Conventional electroless-plating processes are widely used for the coating of metal nanoparticles[26,27] on the surface of pretreated CNFs to achieve uniform density of surface functional groups.[28,29] A few other techniques such as dip-coating in poly(furfuryl alcohol) (PFA) and tetraethylorthosilicate (TEOS) to functionalize CNF surfaces with carbon and silica nanoparticles have also been reported.[30] However, these methods have disadvantages such as severe chemical treatment, long reaction time, high temperatures, and complicated processes resulting in a decrease of the electrical, chemical and mechanical properties.[31]

[a] Carbon Convergence Materials Research Center, Institute of Advanced Composite Materials, Korea Institute of Science and Technology, San 101, Eunha-ri, Bongdoung-eup, Wanju-gun, Jeollabuk-do 565-905, Korea. E-mail: sunghol@kist.re.kr
[b] School of Electrical and Electronic Engineering, Yonsei University, 50 Yonsei-ro, Seodaemun-gu, Seoul 120-749, Republic of Korea
[c] Department of Nano Material Engineering, Korea University of Science and Technology, 217 Gajeong-ro, Yuseong-gu, Daejeon 305-350, Korea
[d] Department of Physics and Astrophysics, University of Delhi, New Delhi-110007, India. E-mail: vgupta@physics.du.ac.in
[e] Department of Physics, Miranda House, University of Delhi, New Delhi-110007, India

† Electronic supplementary information (ESI) available. See DOI: 10.1039/c5tb01781e

In recent years, copper nanoparticles have been studied considerably due to their ease of synthesis, cost effectiveness, good electrical conductivity, and biocompatibility.[32] Hydroxyl ion assisted alcohol reduction is one of the promising methods for the synthesis of metal nanoparticles, which has reasonably low redox potential such as copper.[33] Metal oxide nanoparticles provide a high surface-to-volume ratio and a biocompatible environment for the immobilization of biomolecules and hence, they have been successfully used in the fabrication of various biosensors.[34–36]

The reliable monitoring of the cholesterol concentration in the blood is a considerably important as an increase in cholesterol leads to health disorders.[36] Therefore, cholesterol sensing has been one of the most researched topics,[37] and there is a need for the easy preparation of a robust biosensing platform with the objective of enhancing performance.

In this paper, we demonstrate an easy and one step technique for the coating of CuO nanoparticles on a CNF surface using an alcohol reduction method (dip and heat process) without the use of any strong reducing agents and functional groups. Furthermore, the CuO decorated CNFs were used as an effective matrix to immobilize cholesterol oxidase. In particular, a layer of copper(II) acetate ($Cu(OAc)_2$) nanoparticles was coated on the CNF surface by using a long chain alcohol (1-heptanol) which partially reduces the copper salt and simultaneously initiates the growth of CuO nanoparticles. The uniform growth of CuO was controlled by varying the temperature of 1-heptanol. The morphologies and surface chemical nature of the CNFs and CuO/CNF were investigated by scanning electron microscopy (FE-SEM), X-ray diffraction (XRD) and Raman spectroscopy. The prepared ChOx/CuO/CNF bioelectrode was employed for the detection of cholesterol using electrochemical technique with enhanced performance characteristics.

Experimental

Materials

Polyacrylonitrile (PAN) (M_w = 150 000), copper(II) acetate ($Cu(OAc)_2$), dimethylformamide (DMF) and 1-heptanol were purchased from Sigma Aldrich. Cholesterol oxidase (ChOx) from Streptomyces species was procured from SRL Pvt. Ltd, India, and cholesterol was procured from Sigma-Aldrich. Sodium phosphate monobasic anhydrous and sodium phosphate dibasic dihydrate were obtained from Sisco chemical, India. Sodium chloride (NaCl), potassium ferricyanide ($K_3[Fe(CN)_6]$) and ferrocyanide ($K_4[Fe(CN)_6]$) were acquired from Merck & Co. All the chemicals were used without further purification. Deionized water (resistivity 18.2 MΩ cm) was used in the preparation of aqueous solutions.

Preparation of CNFs

CNFs were prepared by the electrospinning technique using a variable high voltage power supply (Gamma ES40P-20W/DAM) to provide a spinning voltage of 15 kV. Electrospinning solutions were loaded in a 20 ml syringe, to which a stainless steel capillary metal-hub needle was attached. The inner diameter of the metal needle was 0.30 mm. The positive electrode of the high voltage power supply was connected to the needle tip. The grounded electrode was connected to a metallic collector covered with an aluminum foil. The tip to collector distance and the flow rate were fixed at 16 cm and 0.8 ml h^{-1}, respectively. Under a high voltage of 15 kV, a polymer jet was ejected and accelerated toward the counter electrode, while the solvent was rapidly evaporated. Dry fibers were accumulated on the aluminum surface and collected as a fibrous mat. After electrospinning PAN, nanofibers were firstly stabilized in an air environment at 280 °C for 1 h at a heating rate of 5 °C min^{-1} and subsequently carbonized at 1100 °C in a nitrogen atmosphere at a same heating rate.

One step coating with CuO nanoparticles

The supernatant 20 mM solution was prepared by dissolving an exact amount of $Cu(OAc)_2$ in 1-heptanol under mild stirring at 65 °C for 12 h. A layer of a copper precursor was deposited on the surface of the CNF mat and partially reduced by further heating at different temperatures (80, 100, 120, 140 and 160 °C) to initiate the growth of CuO nanoparticles for 1 h. Samples were dried at 60 °C for further processing. Subsequently, the coated CNF mats were sintered at 250 °C at the rate of 5 °C min^{-1} for 2 h under an air atmosphere. A sheet of area 2 cm × 1 cm was utilized for biosensing response studies.

Preparation of bioelectrode

Phosphate buffer saline (PBS) 50 mM, pH 7.0 (0.9% NaCl) solution was prepared by adjusting the proportion of monobasic sodium phosphate solution with dibasic sodium phosphate solution and subsequently adding 0.9% NaCl to the solution. Cholesterol oxidase, ChOx (from Streptomyces species) solution (1 mg ml^{-1}) was freshly prepared in PBS of pH 7.0. The stock solution of cholesterol (analyte) was prepared in 10% Triton X-100 and stored at 4 °C. ChOx was immobilized over the surface of the CuO/CNF sheet by the physical adsorption technique. CuO has a high isoelectric point (~9.5) and ChOx has a low isoelectric point (~4.7). Hence, ChOx can be immobilized by electrostatic interaction on the surface of CuO decorated CNFs. 15 μl of ChOx solution (1 mg ml^{-1}) was spread uniformly over the surface of the CuO/CNFs sheet (1 cm × 1 cm area) and dried at room temperature for 2 h. The prepared bioelectrode (ChOx/CuO/CNFs), was stored at 4 °C overnight and washed with PBS to remove unbound enzyme molecules before use.

Sample characterization

X-ray diffraction analysis (XRD, Smart Lab, Rigaku) of the prepared samples was performed over the 2θ range from 10 to 80°. The operating voltage and current were 45 kV and 200 mA, respectively. The surface morphology of the samples was studied using a field emission scanning electron microscope (FE-SEM, Verios 460 L, FEI) equipped with EDAX (Intec). X-ray photoelectron spectroscopy (XPS) studies (Thermo Scientific, K-alpha) were carried out using monochromatic Al Kα (1486.6 eV) X-rays below a pressure of 3×10^{-7}. The electrical conductivity of

samples was measured by a Loresta-8P, MCP-HT610. Raman spectra were recorded over the range of 100–5000 cm^{-1} using a high resolution Raman spectrometer (LabRAM, HR UV-Visible-NIR). Samples in the form of nanowebs were deposited on a microscope glass slide, and the laser was focused through a 50X microscope objective. Cyclic voltammetry (CV) and electrochemical impedance spectroscopy (EIS) studies were carried out on a Gamry potentiostat/galvanostat (Reference 600) using a three-electrode cell configuration with the Ag/AgCl electrode as a reference electrode, CuO/CNF as the working electrode and platinum foil as a counter electrode. The CV and EIS studies were performed in 10 ml of PBS solution containing 5 mM $K_3[Fe(CN)_6]$.

Results and discussion

CuO nanoparticles were synthesized and coated by the reduction of $Cu(OAc)_2$ with 1-heptanol as shown in Scheme 1. This process was conducted on a small scale in 50 ml of 1-heptanol at different temperatures of 80, 100, 120, 140 and 160 °C for 1 h. The color of the reaction mixture changed with the progression of the reaction, from light green to black to orange. Fig. 1a and b shows the XRD patterns of the CuO/CNF samples synthesized at different temperatures before and after sintering for a fixed reaction time in this process. The XRD pattern of bare CNFs is also included in Fig. 1a and b for comparison. All prepared samples (before and after sintering) synthesized at higher temperatures (≥100 °C) exhibit diffraction peaks of 2θ at

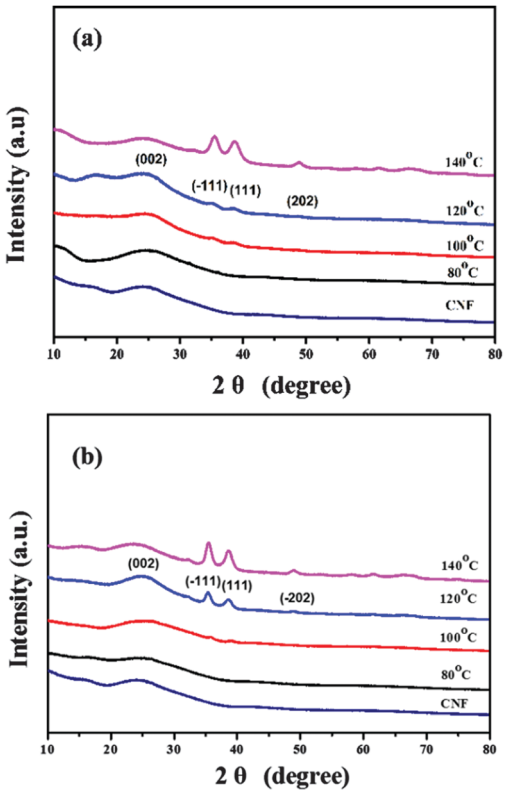

Fig. 1 XRD patterns of metal copper coated CNFs at different reaction temperatures (a) before sintering and (b) after sintering at 250 °C.

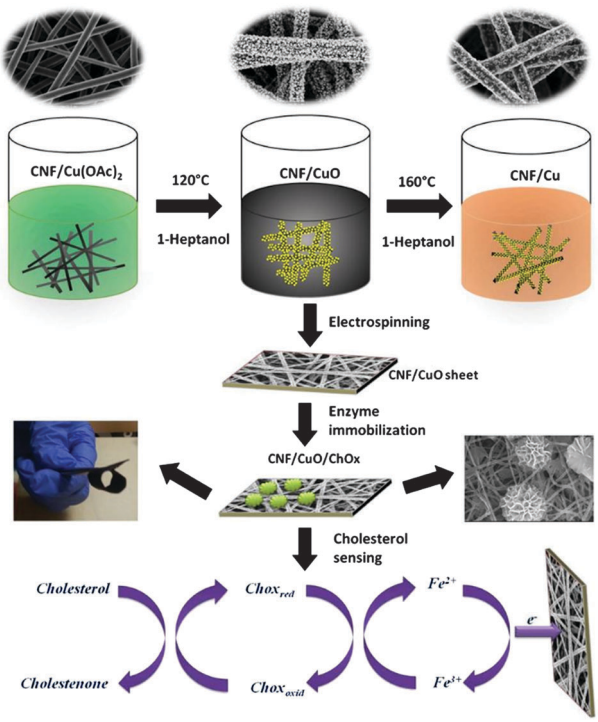

Scheme 1 Schematic illustration of one-step coating of CuO nanoparticles compounds on the surface of CNFs and the preparation of the ChOx/CuO/CNF bioelectrode along with the proposed mechanism of cholesterol biosensing.

35.5, 38.7 and 49.0 associated with (−111), (111) and (−202) crystal planes of the monoclinic phase of CuO (Fig. 1a and b) respectively.[38–40] However, the intensities of the diffraction peaks are clearer and higher in the case of samples which were sintered at 250 °C for 2 h under an air atmosphere as shown in Fig. 1b.

On the other hand, a flake of copper oxide starts to be produced when temperature was 140 °C. Furthermore, at 160 °C the diffraction peaks are dramatically decreased, due to metal phase formation of copper nanoparticles within the solution. Therefore, very few metal ions were coated on the surface of CNFs and no significant peaks appeared at this temperature. The broad diffraction peaks observed at moderate temperature in the present study indicate that CNFs are decorated with CuO particles of small size.[41] SEM images of the surface of the bare CNF sample and the CuO coated CNF sample prepared at 120 °C are shown in Fig. 2a and b respectively. It is clearly seen from Fig. 2a that all carbon nanofibers are of uniform diameter and randomly oriented, forming an interwoven network on the substrate. The interwoven structures are increasing the facility for the intercalation of the metal precursor with the CNF surface, while processing CuO nanoparticles. Therefore, copper oxide nanoparticles are uniformly coated on the surface of CNFs at an optimized temperature of 120 °C (Fig. 2b). The average particle size of the deposited CuO on the CNF surface in the temperature range from 100 to 120 °C is 20 to 40 nm (Fig. 2b; also see Fig. S1b in the ESI†). Interestingly, when the

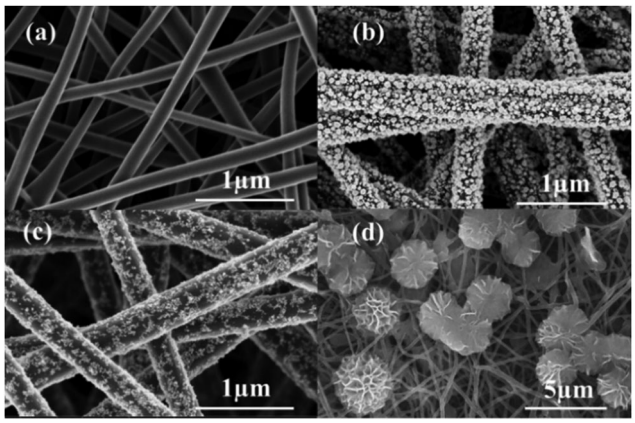

Fig. 2 SEM images of CuO decorated CNFs: (a) pure CNF, (b) 120 °C, (c) 160 °C, (d) ChOx-immobilized.

processing temperature was increased to 140 °C, the coating of CuO nanoparticles on the surface of the CNFs was decreased (Fig. S1c in ESI†). In addition, at much higher temperature (160 °C) the deposition of CuO nanoparticles is dramatically decreased and found to be randomly placed on the surface of the CNFs (Fig. 2c). The above results indicate that with increase in temperature the reduction of copper acetate has been increased by 1-heptanol and self-agglomeration into the solution resulted in less coating on the surface of CNFs. In contrast, at a lower temperature of 80 °C a low content of CuO is deposited on the surface of the CNFs due to the low reduction rate of 1-heptanol (see Fig. S1a in the ESI†).

The SEM analysis of the prepared samples is in good agreement with the XRD data. Since biosensing is a surface dominating phenomenon, the interwoven network of CNFs having CuO nanoparticles on their surface is advantageous for biosensing applications. The presence of CuO nanostructures offers a high surface-to-volume ratio and hence provides a larger surface area for enzyme immobilization.[42] Further, it is worth noting that CNFs are coated with monoclinic CuO, which exhibits good electron transfer properties and is important for the development of an efficient biosensor with enhanced response.[49] It may be noted that the CuO/CNF sample prepared at 120 °C has a large amount of CuO nanoparticles on its surface, therefore, the sample (CuO/CNF-120) has been considered for further study for biosensing applications. Fig. 2d shows the surface morphology of the surface of the CuO/CNF sample prepared at 120 °C after immobilization of cholesterol oxidase (ChOx). The presence of large globular structures in the SEM image (Fig. 2d) confirms the successful immobilization of ChOx on the surface of the CuO decorated CNF sample *via* electrostatic interaction. EDAX analysis of the CuO decorated CNFs processed at 80 °C, 100 °C, 120 °C, 140 °C, and 160 °C can be found in Fig. S2 in the ESI.†

In order to understand the mechanism of the surface modification process due to loading of CuO nanoparticles on CNFs, the surface chemistry of CuO/CNF-120 was studied by X-ray photoelectron spectroscopy (XPS) and the XPS spectra are shown in Fig. 3a. The XPS spectra of the bare CNF sample are

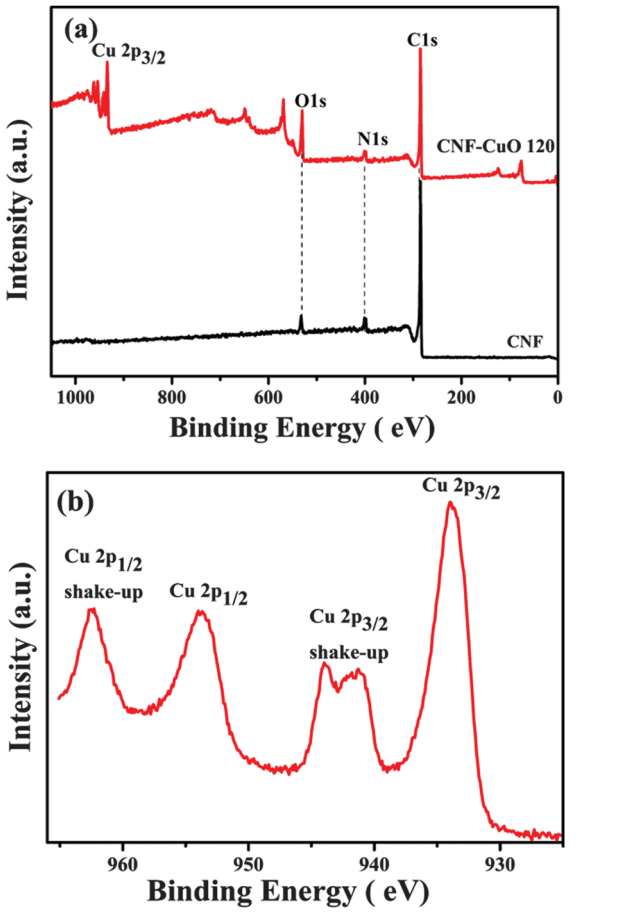

Fig. 3 (a) XPS survey scans of bare CNF and CNF/CuO-120 samples, and (b) the expanded XPS spectrum for the CNF/CuO-120 sample in the Cu_{2p} region.

also shown in Fig. 3a and peaks corresponding to only C1s, N1s and O1s are visible at 284.5 eV, 397.5 eV and 531.9 eV respectively in the XPS spectra of the bare CNF sample (Fig. 3b). After treatment of CNFs with a supernatant solution of $Cu(OAc)_2$/1-heptanol at 120 °C, the presence of an additional peak, namely $Cu2p_{3/2}$ at 933.8 eV is observed in the XPS spectra (Fig. 3a), indicating the coating of CuO on the CNF surface. Furthermore, an increase in the intensity of the peak corresponding to oxygen (O1s) was noted for the CuO/CNF-120 sample in comparison to that obtained for the bare CNF sample (Fig. 3a). Detailed studies of the C1s core level further confirm the presence of CuO on the surface of the CNFs. The presence of an oxygen functional group from 1-heptanol makes the CNFs hydrophilic and supports good adhesion of CuO nanoparticles on their surface.[32] The expanded XPS spectrum of the CuO/CNF-120 sample in the Cu_{2p} region is shown in Fig. 3b.

XPS peaks were observed corresponding to $Cu_{2p3/2}$ and $Cu_{2p1/2}$ at binding energies of 934.2 eV and 954.1 eV respectively (Fig. 3b). Furthermore, the shake-up satellite peaks of $Cu_{2p3/2}$ and $Cu_{2p1/2}$ at 942.4 and 962.6 respectively confirmed the formation of Cu^{2+} on the surface of the CNFs.[40] In order to confirm the presence of CuO on the CNF surface, the Raman spectra for both bare CNF and CuO/CNF-120 samples were also recorded at

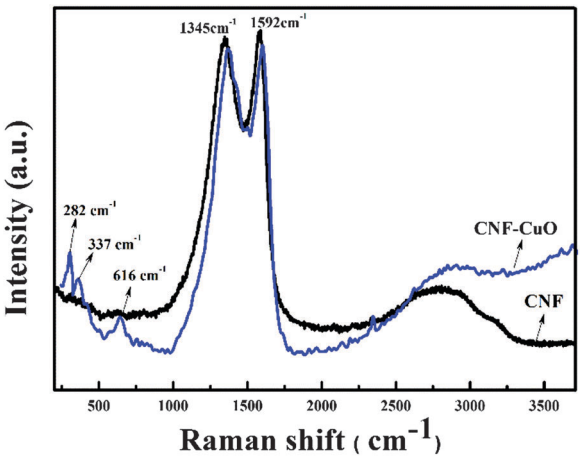

Fig. 4 Raman spectra of bare CNF and CNF/CuO-120 samples.

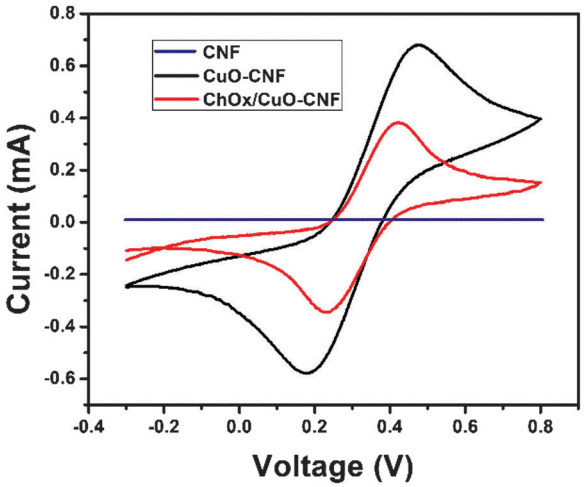

Fig. 5 Cyclic voltammograms of bare CNF, CuO/CNF-120 and ChOx/CuO/CNF-120 electrodes in PBS solution containing the $[Fe(CN)_6]^{3-/4-}$ mediator.

room temperature in back scattering configuration and are shown in Fig. 4. Sharp and well defined phonon modes around 1345 and 1580 cm^{-1} have been observed for the bare CNF sample (Fig. 4). Additional phonon modes at around 282, 330 and 616 cm^{-1} have been obtained for the CuO/CNF-120 sample (Fig. 4), confirming the deposition of CuO nanoparticles on the surface of the CNFs.[42] The mode observed at 282 cm^{-1} is assigned to A_g and the modes at 337 and 616 cm^{-1} are assigned to the B_g modes.[43] These modes are in close agreement with those reported in the literature by other workers.[42,43]

As discussed earlier, the reaction temperature significantly influences the synthesis and coating of copper nanoparticles on the surface of CNFs, which in turn may affect the electrical properties of the CuO/CNF composite samples. The electrical conductivity measurements of CuO/CNF-120 and bare CNF samples have been studied using the four probe method and the obtained results are shown in Table S1 (ESI†). The value of electrical conductivity for the CNF/CuO-120 sample prepared at 120 °C is found to be around 251 S m^{-1}, which is relatively low in comparison to the corresponding value (473 S m^{-1}) obtained for the CNF sample. The observed decrease in electrical conductivity is attributed to the presence of oxygen moieties on the surface of the CNFs after integration of CuO nanoparticles. The electrochemical properties of the bare CNF, CuO/CNF-120 and ChOx immobilized CuO/CNF-120 (ChOx/CuO/CNF) electrodes were studied using cyclic voltammetry (CV) in PBS solution containing the $[Fe(CN)_6]^{3-/4-}$ mediator, which provides the redox couple. The obtained CV spectra for all these electrodes are shown in Fig. 5. It is important to note that the bare CNF sample does not show any oxidation or reduction peaks in the CV response (Fig. 5). However, when the CNFs were decorated with CuO nanoparticles (CuO/CNF-120), a well-defined CV curve with oxidation and reduction peaks was observed. The results obtained clearly indicate that the presence of CuO nanoparticles results in enhanced electron transfer kinetics of the CuO/CNF-120 electrode. The peak oxidation current (Ipo) of the CuO/CNF-120 electrode was found to decrease from 0.68 mA to 0.37 mA following the immobilization of an enzyme (ChOx) on its surface (Fig. 5) and is attributed to the insulating nature of the macromolecule which hinders electron transfer. Cyclic voltammograms of the ChOx/CuO/CNF-120 bioelectrode recorded at different scan rates (80 to 170 mV s^{-1}) are shown in Fig. 6. It can be seen from Fig. 6 that the anodic potential (Epo) shifts continuously towards higher potential values, while the cathodic peak potential (Epr) shifts in the reverse direction (Fig. 6) implying the quasi-reversibility of the prepared system.

However, the redox peak currents are proportional to the square root of the scan rate ($\nu_{1/2}$) as shown in Fig. 7, indicating a diffusion assisted electron-transfer process in the present work.

The EIS curves were recorded in the frequency range of 0.01–10^5 Hz and modelled according to the Randles circuit which includes the capacitance of the dielectric layer (C_{DL}) in series with the electrolyte resistance (R_S), the charge-transfer resistance (R_{CT}), and the Warburg impedance (Z_W) as shown in Fig. 8a. The semicircle part, observed at higher frequencies, is associated

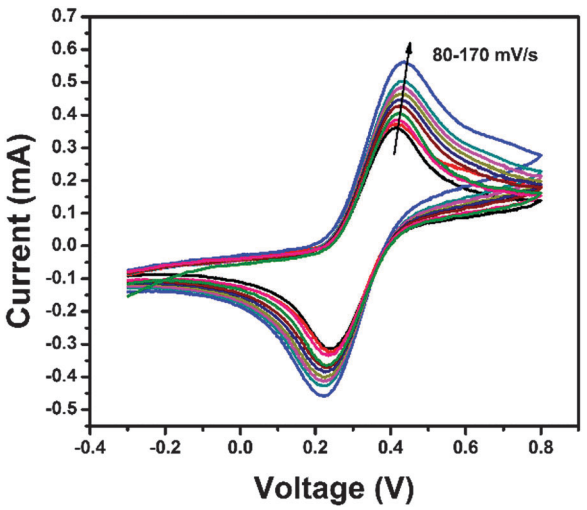

Fig. 6 Effect of the scan rate on the CV response of the ChOx/CuO/CNF-120 bioelectrode.

with the electron transfer limited process, while the linear part seen at lower frequencies is characteristic of a diffusion limited process. The value of the charge transfer resistance, R_{CT}, was found to be approximately 26 Ω for the composite, highlighting its excellent charge transfer characteristics. Upon immobilization of the enzyme, this value increased to 46 Ω due to the insulating nature of the enzyme over the surface of the CuO/CNF sheet which is in accordance with the CV studies. The EIS of a pure CNF sheet has also been included for comparison. However, the typical semicircle behavior was not observed at higher frequencies for the pure CNF sheet. An almost straight line was seen, suggesting a diffusion-limited process (Fig. 8a). Electrochemical response studies of the prepared bioelectrode (ChOx/CuO/CNF-120) were carried out as a function of cholesterol concentration (0.12 mM to 12.93 mM) and the corresponding CV spectra are shown in Fig. 8b. The peak oxidation current (Ipo) gradually increases linearly from 0.52 mA to 1.48 mA with an increase in cholesterol concentration from 0.12 mM to 12.93 mM. The observed increase in peak oxidation current with increasing cholesterol concentration is due to the biochemical reaction occurring at the surface of the bioelectrode between the analyte and immobilized ChOx. This indicates that the prepared bioelectrode had excellent sensitivity to cholesterol. ChOx immobilized on the bioelectrode surface catalyzes the oxidation of cholesterol (analyte) in the PBS solution to 5-cholest-3-one and itself gets reduced. It gets reoxidized by donating excess electrons to the $[Fe(CN)_6]^{3-}$ species (mediator) present in the PBS solution which on oxidation generate electrons. These electrons are accepted by the CuO/CNF-120 matrix which provides a fast electron communication path towards the electrode leading to an increase in oxidation current with cholesterol concentration. The sensitivity of the prepared biosensor (ChOx/CuO/CNF-120) towards cholesterol has been calculated from the slope of the calibration curve (see Fig. 8c) and is found to be about 75 μA mM^{-1} cm^{-2}. The sensitivity observed in the present work is higher than the corresponding values reported by various studies using other matrices (Table 1).

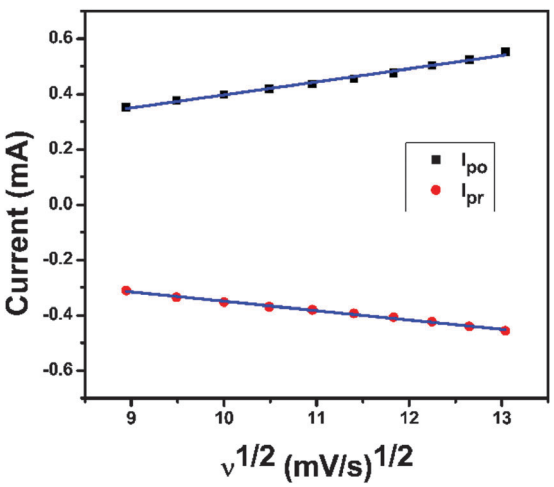

Fig. 7 Variation of peak oxidation and reduction currents as a function of square root of scan rate.

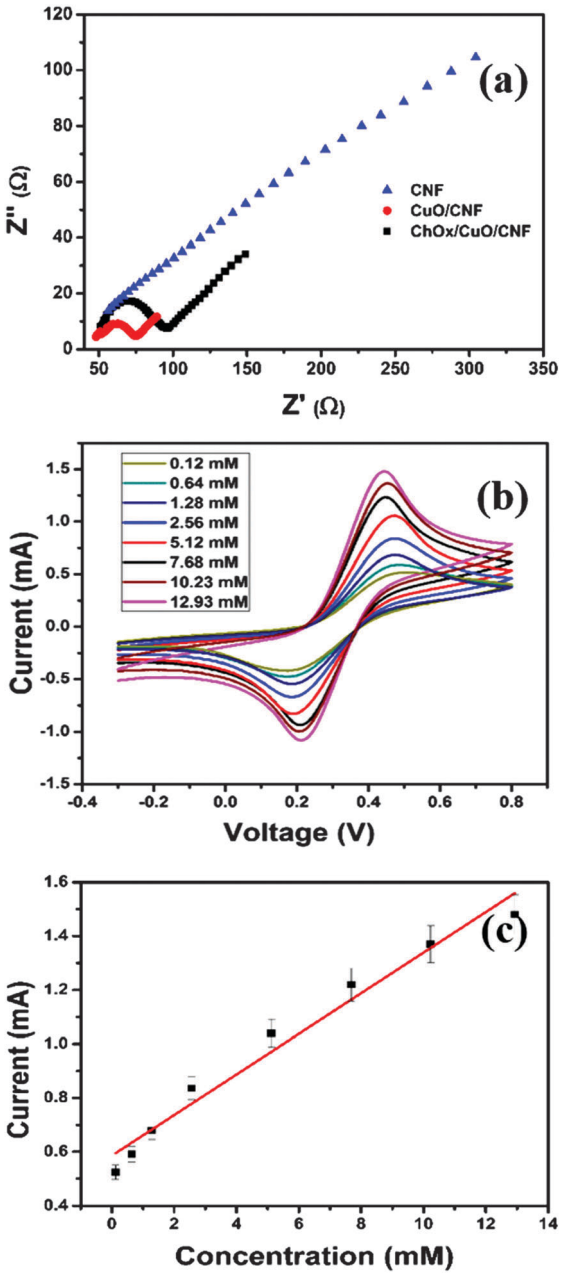

Fig. 8 (a) EIS curves of the pure CNF, the CuO/CNF sheet and the ChOx/CuO/CNF bioelectrode (b) CV spectra of the ChOx/CuO/CNF-120 bioelectrode with an increase in cholesterol concentration from 0.12 mM to 12.93 mM, and (c) variation in peak oxidation current as a function of cholesterol concentration.

In order to demonstrate the flexibility of the sensor, CV curves were recorded under three different conditions: without bending, moderate bending (45°) and complete bending (90°). The peak oxidation current, and hence, the sensitivity was found to decrease to some extent with increase in bending (Table S2 in the ESI†). The measurements were repeated five times for each bending configuration and the results were found to be reproducible within ±5%. It is important to note that the current returned to its previous value when the bending was released and the sheet was in flat condition (no bending).

Table 1 Comparison of sensing characteristics of the present biosensor along with other reports

Matrix	Flexibility	Sensitivity ($\mu A\ mM^{-1}\ cm^{-2}$)	Linear range (mM)	Shelf life	Ref.
$NiFe_2O/CuO/FeO$–chitosan	Not flexible	16.54	0.13–12.95	3 months	Singh *et al.*[44] (2012)
Pt–Au/ZnO nanorods–MWCNT	Not flexible	26.8	$\leq$7.59	4 weeks	Wang *et al.*[45] (2012)
ZnO	Not flexible	56	0.64–12.93	12 weeks	Batra *et al.*[46] (2013)
Polyaniline–Au–chitosan	Not flexible	33	1.29–12.23	3 weeks	Srivastava *et al.*[47] (2014)
Graphene/polyvinylpyrrolidone/polyaniline nanocomposite	Flexible	34	0.05–10	2 weeks	Ruecha *et al.*[48] (2014)
CuO/CNF	Flexible	75	0.12–12.93	6 weeks	Present work

The Michaelis Menten constant (K_M) was calculated from the Hanes plot *i.e.* the graph between [analyte concentration/peak oxidation current] and [analyte concentration] (see Fig. S3 in the ESI†). The value of K_M was estimated to be about 1.42 mM. A low value of K_M signifies higher interaction of the immobilized enzyme (ChOx) with the analyte (cholesterol) and hence, higher catalytic efficiency. The shelf-life of the bioelectrode is studied by measuring the sensing response at regular intervals over a span of 6 weeks and the bioelectrode retains about 95% of its response. The selectivity test was performed for the biosensor by measuring the peak oxidation current in CV on addition of normal interferents present in human serum such as glucose (5 mM), uric acid (0.1 mM), urea (1 mM), lactic acid (0.5 mM) and ascorbic acid (0.05 mM) in buffer solution along with cholesterol (5.12 mM). The concentrations of different interferents have been chosen based on their normal levels in human serum. The maximum interference was found to be less than $\pm$3% and hence, the biosensor is selective towards cholesterol (Fig. S4 in the ESI†).

It may be noted from Table 1 that the prepared biosensor in the present work exhibits an enhanced response ($75\ \mu A\ mM^{-1}\ cm^{-2}$) over a wide linear concentration range (0.12 to 12.93 mM) of cholesterol with a good shelf life besides being flexible in nature. The excellent performance characteristics of the prepared biosensor may be due to higher enzyme loading owing to the presence of CuO nanoparticles on the surface of the CNF matrix. Earlier reports on cholesterol sensors based on different nanocomposites showed good performance,[46–48] but flexibility of a substrate was the major concern as indicated in Table 1. To validate the fabricated biosensor, its testing was done in real human serum samples (Table S3 in the ESI†). However, it is important to note that cholesterol is found in blood in free form (about 30% of the total content) or as cholesterol esters (approximately 70% of the total content). The laboratory value of free cholesterol is generally not available but its value is approximately 30% of the total cholesterol content in all the cases. The biosensor needs to be modified in order to check the total cholesterol levels by immobilizing both enzymes, cholesterol esterase and cholesterol oxidase on the surface of the matrix. The results indicate that the cholesterol concentration in the serum determined using the developed biosensor agreed well with the spectrophotometric data obtained from the laboratory tests. Real samples were then spiked with a known concentration (2.56 mM) of cholesterol and recovery tests for cholesterol were performed. The amounts of added cholesterol were then evaluated by using the fabricated biosensor. These results demonstrate that the developed biosensor is accurate and precise and its performance is comparable with the commercially accepted methods.

Conclusions

The aim of the study was to obtain a uniform coating of CuO nanoparticles on the surface of CNFs and to fabricate flexible substrates for biosensing. We have successfully demonstrated that 1-heptanol can be used for one step coating of CuO nanoparticles on the surface of CNFs without using any external reducing agent. A reaction temperature between 100 and $\sim$140 °C is suitable for synthesis and coating. The CuO/CNF was utilized as a biosensing matrix for the detection of cholesterol with a high sensitivity ($75\ \mu A\ mM^{-1}\ cm^{-2}$) and linearity. Our proposed method is highly effective as compared to other conventional metal coating technologies for CNFs and provides a better shelf life (6 weeks) to the substrate. The 3-D interwoven nanofiber structure also supports a higher immobilization rate of biomolecules on the surface of CNFs. These CuO coated CNF bio-substrates are advantageous over conventional substrates because of their flexible structure which can be used for easy biomedical instrumentation. It can further reduce the space, weight, complexity and cost of the system by integrating electronics into the physical structure and enables the construction of lightweight and durable devices that can be rolled up or folded when not in operation. This coating method offers easy and inexpensive processing along with a robust supporting structure for biosensing applications.

Acknowledgements

This work was supported by the Korea Institute of Science and Technology (KIST) Program.

References

1 S. Chand, *J. Mater. Sci.*, 2000, **35**, 1303.
2 Y. Qin, X. D. Wang and Z. L. Wang, *Nature*, 2008, **451**, 809.
3 C. A. Bonino, L. W. Ji, Z. Lin, O. Toprakci, X. W. Zhang and S. A. Khan, *ACS Appl. Mater. Interfaces*, 2011, **3**, 2534.
4 H. Kim, X. Huang, X. Guo, Z. Wen, S. Cui and J. Chen, *ACS Appl. Mater. Interfaces*, 2014, **6**, 18590.
5 K. P. DeJong and J. W. Geus, *Catal. Rev.: Sci. Eng.*, 2001, **42**, 481.

6 N. M. Barakat, M. El-Newehy, S. Al-Deyab and H. Y. Kim, *Nanoscale Res. Lett.*, 2014, **9**, 2.
7 Y. Z. Wu, M. V. Reddy, B. V. R. Chowdari and S. Ramakrishna, *ACS Appl. Mater. Interfaces*, 2013, **5**, 12175.
8 M. Tsuji, M. Kubokawa and R. Yano, *Langmuir*, 2007, **23**, 387.
9 X. Tao, X. Zhang and L. Zhang, *Carbon*, 2000, **44**, 1425.
10 V. Vamvakaki, T. Katerina and N. Chaniotakis, *Anal. Chem.*, 2006, **78**, 5538.
11 S. Demirci Uzun, F. Kayaci, T. Uyar, S. Timur and L. Toppare, *ACS Appl. Mater. Interfaces*, 2014, **6**, 5235.
12 L. Dawei, L. Lei, P. Zengyuan, D. Lei, W. Qingqing, K. Huizhen, H. Fenglin and W. Qufu, *ACS Appl. Mater. Interfaces*, 2014, **6**, 5144.
13 A. Rengaraj, Y. Haldorai, C. H. Kwak, S. Ahn, K. Jeon, S. H. Park, Y. Han and Y. S. Huh, *J. Mater. Chem. B*, 2015, **3**, 6301.
14 G. G. Wildgoose, C. E. Banks and R. G. Compton, *Small*, 2006, **2**, 182.
15 Y. B. Li, B. Q. Wei, C. L. Xu, J. Jiang and D. H. Wu, *J. Mater. Sci.*, 1999, **34**, 5281.
16 J. M. Gomez-de-Salazar, M. I. Barrena, C. Merino and N. Merino, *Mater. Lett.*, 2008, **62**, 494.
17 T. W. Ebbesen, H. Hiura and M. E. Bischer, *Adv. Mater.*, 1996, **8**, 155.
18 B. C. Satishkumar, E. M. Vogl, A. Govindaraj and C. N. R. Rao, *J. Phys. D: Appl. Phys.*, 1996, **29**, 3173.
19 S. Rana, R. Alagirusamy, R. Fangueiro and M. Joshi, *J. Appl. Polym. Sci.*, 2015, **125**, 1951.
20 J. S. Yu, S. Kang, S. B. Yoon and G. Chai, *J. Am. Chem. Soc.*, 2002, **124**, 9382.
21 W. Z. Li, C. H. Liang, W. J. Zhou and Q. Xin, *J. Phys. Chem. B*, 2003, **107**, 6292.
22 G. Che, B. B. Lakshmi, C. R. Martin and E. R. Fisher, *Langmuir*, 1999, **15**, 750.
23 S. H. Joo, S. J. Choi, I. Oh, J. Kwak and Z. Liu, *Nature*, 2001, **412**, 169.
24 Z. Liu, X. H. Lin, J. Y. Lee, W. Zhang and M. Han, *Langmuir*, 2002, **18**, 4054.
25 R. Q. Yu, L. W. Chen and Q. P. Liu, *Chem. Mater.*, 1998, **10**, 718.
26 B. Bajaj, S. H. Lee, S. J. Yoon, B. H. Park, B. Kim and B. K. Park, *J. Mater. Chem.*, 2012, **22**, 2975.
27 B. Bajaj, B. Kim, S. J. Yoon, B. K. Park and J. R. Lee, *Fibers Polym.*, 2014, **15**, 47.
28 R. L. Meek, *J. Electrochem. Soc.*, 1975, **122**, 1478.
29 B. K. W. Baylis, A. Busuttil, N. E. Hedgecock and M. Schlesinger, *J. Electrochem. Soc.*, 1976, **123**, 348.
30 Y. Zhang and A. L. Yarin, *Langmuir*, 2011, **27**, 14627.
31 I. Kiflawick and M. Schlesinger, *J. Electrochem. Soc.*, 1983, **130**, 872.
32 J. Fu, H. Qiao, D. Li, L. Luo, K. Chen and Q. Wei, *Sensors*, 2014, **14**, 3543.
33 J. C. Huaman, K. Sato, S. Kurita, T. Matsumoto and B. Jeyadevan, *J. Mater. Chem.*, 2011, **21**, 7062.
34 P. R. Solanki, A. Kaushik, V. V. Agrawal and B. D. Malhotra, *NPG Asia Mater.*, 2011, **3**, 17.
35 M. Tyagi, M. Tomar and V. Gupta, *Biosens. Bioelectron.*, 2013, **41**, 110.
36 K. Arora, M. Tomar and V. Gupta, *Biosens. Bioelectron.*, 2011, **30**, 333.
37 K. Mondal, M. A. Ali, V. V. Agarwal, B. D. Malhotra and A. Sharma, *ACS Appl. Mater. Interfaces*, 2014, **6**, 2516.
38 M. Gopiraman, S. G. Babu, Z. Khatri, W. Kai, Y. A. Kim, M. Endo, R. Karvembu and I. S. Kim, *Carbon*, 2013, **62**, 135.
39 P. Zhang, L. Zhang, G. Zhao and F. Feng, *Microchim. Acta*, 2012, **176**, 411.
40 C. C. Chusei, M. A. Brookshier and D. W. Goowdman, *Langmuir*, 1999, **15**, 2806.
41 N. Batra, M. Tomar and V. Gupta, *Analyst*, 2012, **137**, 5854.
42 M. Rashad, M. Rüsing, G. Berth, K. Lischka and A. Pawlis, *J. Nanomater.*, 2013, **714853**, 1.
43 J. Xu, J. W. Ji, Z. Shen, W. S. Li, S. H. Tang, X. R. Ye, D. Z. Jia and X. Q. Xin, *J. Raman Spectrosc.*, 1999, **30**, 413.
44 J. Singh, M. Srivastava, K. Prasanta and B. D. Malhotra, *Process Biochem.*, 2012, **47**(12), 2189.
45 C. Wang, X. Tan, S. Chen, R. Yuan, F. Hu, D. Yuan and Yu. Xiang, *Talanta*, 2012, **94**, 263.
46 N. Batra, M. Tomar and V. Gupta, *J. Exp. Nanosci.*, 2013, **8**, 280.
47 M. Srivastava, S. K. Srivastava, N. R. Nirala and R. A. Prakash, *Anal. Methods*, 2014, **6**, 817–824.
48 N. Ruecha, R. Rangkupan, N. Rodthongkum and O. Chailapakul, *Biosens. Bioelectron.*, 2014, **52**, 13.
49 K. Jindal, M. Tomar and V. Gupta, *Biosens. Bioelectron.*, 2012, **38**, 11–18.

